ISSN 2664-9969

UDC 621.311
DOI: 10.15587/2706-5448.2024.313937

Henrikh Polshchikov,
Pavlo Zhukov

CONSTRUCTION OF A GENERALIZED MATHEMATICAL MODEL AND FAST CALCULATIONS OF PLANE-PARALLEL ROTATING MAGNETIC FIELDS IN PROCESS REACTORS WITH LONGITUDINAL CURRENTS OF CYLINDRICAL INDUCTORS ON A GRAPHICAL CALCULATOR

The object of research is a quasi-stationary rotating magnetic field (RMF) generated by cylindrical inductors with longitudinal windings in the working space of process reactors, in particular reactors designed to work with magnetic particles (MP). The RMF theory in the working space of reactors has not yet been sufficiently developed, which hinders the widespread introduction of the considered, rather complex technologies into practice. The RMF of a specific reactor can be calculated accurately and completely using modern programs based on the finite element method, but it does not replace the general theory and theoretical analysis. In the literature, special cases of circular and elliptical plane-parallel RMF in reactors of the type under consideration have been studied, however, analytical formulas for a plane-parallel RMF for the general case of m-phase cylindrical inductors of external and internal design with symmetrical longitudinal windings are not presented.

In this paper, a mathematical model is constructed and generalized analytical formulas for magnetic induction are obtained, linking the characteristics of a plane-parallel RMF in the working space of reactors at idle speed with the main parameters of external and internal cylindrical inductors with an m-phase symmetric longitudinal winding. A physical analysis is carried out and the adequacy of the model is confirmed. Using the proposed formulas and a free, easy-to-use Desmos graphical calculator, quick trial calculations and analysis of RMF in several reactors with two-pole external inductors and various windings for three phases (for 6 and 42 slots) and for six phases (12 slots) are carried out. The calculation results are consistent with experimental and literary data.

New analytical formulas, as well as the demonstrated methods of quick evaluation calculations, analysis and experimental studies are recommended for practical implementation in the research, development and operation of reactors of this type. To carry out the calculations, it is enough to have a laptop or smartphone connected to the Internet, the time costs are insignificant. The results of the work will be useful to technologists, engineers and developers of both the reactors of the type under consideration and other devices with a similar purpose with an RMF.

Keywords: *rotating magnetic field inductors, circular and elliptical magnetic field, magnetic drive of small particles, reactors with magnetic particles.*

Received date: 03.09.2024
Accepted date: 23.10.2024
Published date: 29.10.2024

How to cite
Polshchikov, H., Zhukov, P. (2024). Construction of a generalized mathematical model and fast calculations of plane-parallel rotating magnetic fields in process reactors with longitudinal currents of cylindrical inductors on a graphical calculator. Technology Audit and Production Reserves, 5 (1 (79)), 38–49. https://doi.org/10.15587/2706-5448.2024.313937

1. Introduction

Magnetic particle (MP) reactors using the rotating magnetic field (RMF) of cylindrical inductors with longitudinal AC windings are used in a wide range of industrial and scientific applications [1–9]. However, their theory, including the RMF theory of cylindrical inductors, has not yet been sufficiently developed. The RMF of a specific reactor can be calculated accurately and completely using modern programs based on the finite element method, but it does not replace the general theory and theoretical analysis.

Previously, analytical expressions were obtained and studied that describe various types of circular RMF of idealized external cylindrical inductors with a sinusoidal longitudinal winding [10], as well as plane-parallel elliptical RMF of three-phase external inductors with a symmetrical longitudinal winding [11].

Generalized analytical formulas for the plane-parallel RMF for *m*-phase cylindrical inductors of external and internal design with symmetrical longitudinal windings have not yet been presented in the literature.

The aim of research is to derive and analyze the above-mentioned formulas with subsequent examples of their application and confirmation of adequacy.

The work will be useful to researchers, technologists and engineers for the prompt assessment and analysis of the RMF characteristics and the parameters of the inductors in the process of designing and operating various reactors.

2. Materials and Methods

Reactors with cylindrical inductors of two types are considered:

1) a reactor with an external inductor similar to the stator of an electric machine, with a boring radius r_0;

2) a reactor with an internal inductor similar to a stationary rotor of an electric machine with a phase winding and a turning radius r_0.

The working chamber and the medium in the reactor at this stage of the research are assumed to be non-magnetic and non-conductive.

The boundary value problem for describing a plane-parallel quasi-stationary RMF reactor is solved in polar coordinates with an answer obtained in the form of an expansion of the components of the magnetic induction vector in a Fourier series. The boundary conditions are specified by the values of the tangential, i. e. tangent to the boundary, component of the magnetic induction vector, which determines the distribution of the magnetic potential along the boundary. Therefore, the boundary value problem solved here has all the features of the Dirichlet problem, which, in particular, means the uniqueness of the solution to the problem. The problem is solved by superimposing the fields of the coils of an *m*-phase symmetrical winding with a number of pole pairs. The general principles of constructing windings of electrical machines are taken into account: the coil is limited by the limits of the pole division; the coils can be connected into a coil group with a constant displacement of adjacent coils; there can be several coil groups in a phase. The magnetic field from the coil current, from the coil group current, from the current of a single-phase, *m*-phase winding is described sequentially.

Measurements of the magnetic induction components were carried out using miniature induction sensors in the normal operating mode of the inductors. Miniature two-coordinate induction sensors were made to measure the phase shift and induction hodographs.

Calculations and graphs were performed using the Desmos graphic calculator.

3. Results and Discussion

The boundary value problem of describing the working RMF of both external and internal inductors is considered under the same boundary conditions on the core surface $r=r_0$.

Assumptions: the inductors are infinitely long; the inductor cores have infinitely high magnetic permeability and infinitely low electrical conductivity; the magnetic field is quasi-stationary; the variability of the boundary value on the surface in the slot section can be neglected; the winding is symmetrical.

Main designations: r_0 – the core surface radius; p – the number of pole pairs; ω – the frequency of the power supply network; m – the number of phases; q – the number of coils in the coil group; θ – the angle characterizing the displacement of the coils in the coil group; β – the relative coil pitch; ρ – the half the slot opening angle; Iw – the coil ampere turns.

3.1. Magnetic field of a coil with current. The polar coordinates (r, α) in the plane of the inductor cross-section with the pole on the inductor axis and the origin of the angle α on the coil axis are used. The boundary conditions on the core surface $r=r_0$ are specified by one of the known methods [12] – the values of the tangential component $B_{0\alpha}$ of the magnetic induction vector $\bar{B}$, and are shown in Fig. 1.

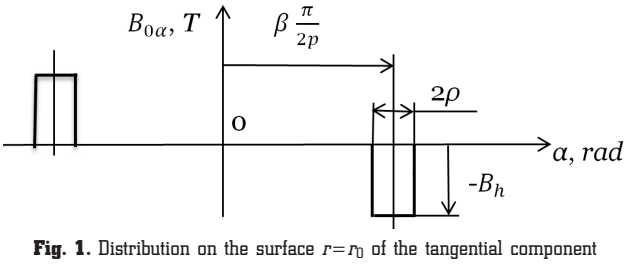

Fig. 1. Distribution on the surface $r=r_0$ of the tangential component of the induction vector of the magnetic field of a coil with current: π/p – the diametrical pitch of the coil (pole division of the inductor), β – the relative pitch of the coil, 2ρ – the opening angle of the slot with the coil current

Such boundary conditions are valid for the surface of an infinite ferromagnetic tube and in most practical cases are approximately fulfilled for the surface of the inductor core, in the slots of which the longitudinal winding coil is placed. The dependence $B_{0\alpha}(\alpha)$ is an odd function. The value of the tangential component of the magnetic induction vector is determined by the ampere turns Iw of the section 2ρ:

$$B_h = \mu_0 \frac{Iw}{2\rho r_0}, \quad (1)$$

where $\mu_0 = 4\pi\cdot 10^{-7}$ H/m – the magnetic constant, I – the coil current, w – the number of coil turns.

After decomposition of the function shown in Fig. 1 functions in a Fourier series:

$$B_{0\alpha} = \sum_{k=1}^{\infty} b_k \sin k\alpha,$$

$$b_k = \frac{2}{\pi}\int_0^{\pi} B_{0\alpha}(\alpha)\sin k\alpha \mathrm{d}\alpha =$$

$$= -\frac{2}{\pi}B_h \int_{\frac{\beta\pi}{2p}-\rho}^{\frac{\beta\pi}{2p}+\rho} \sin k\alpha \mathrm{d}\alpha = -\frac{2}{\pi k}B_h \int_{\left(\frac{\beta\pi}{2p}-\rho\right)k}^{\left(\frac{\beta\pi}{2p}+\rho\right)k} \sin k\alpha \mathrm{d}(k\alpha) =$$

$$= \frac{2}{\pi k}B_h\left(\cos\left(\frac{\beta\pi}{2p}+\rho\right)k - \cos\left(\frac{\beta\pi}{2p}-\rho\right)k\right) =$$

$$= \frac{2}{\pi k}B_h 2\sin\left(k\frac{\beta\pi}{2p}\right)\sin(-k\rho) = -\frac{4\rho}{\pi}B_h k_{\beta k} k_{\rho k}, \quad (2)$$

ISSN 2664-9969

obtained:

$$B_{0\alpha} = -\frac{4\rho}{\pi} B_h \sum_{k=1}^{\infty} k_{\beta k} k_{\rho k} \sin k\alpha; \quad (3)$$

$$k_{\beta k} = \sin\left(k\frac{\beta\pi}{2p}\right); \quad (4)$$

$$k_{\rho k} = \frac{\sin k\rho}{k\rho}, \quad (5)$$

where $k_{\beta k}$ – the shortening factor of the coil winding (coil pitch) of the k-th member of the series; $k_{\rho k}$ – the slot opening factor or the width of the current sheet of the k-th member of the series [11, 13].

Based on the laws of the potential field, it is possible to assume that:

$$B_{0r} = \pm\frac{4\rho}{\pi} B_h \sum_{k=1}^{\infty} k_{\beta k} k_{\rho k} \cos k\alpha. \quad (6)$$

Further, in the combinations of signs "±", "∓", the upper sign is assigned to the variant based on the "plus" in (6), the lower one – to the variant based on the "minus" in (6).

According to the theory of potential electromagnetic field:

$$div\vec{B} = \frac{1}{r}\left(\frac{\partial(rB_r)}{\partial r} + \frac{\partial B_\alpha}{\partial\alpha}\right) = 0, \quad (7)$$

$$|rot\vec{B}| = \frac{1}{r}\left(\frac{\partial(rB_\alpha)}{\partial r} - \frac{\partial B_r}{\partial\alpha}\right) = 0. \quad (8)$$

To solve the problem using the well-known method of separating variables, it is possible to assume:

$$B_r = \pm\sum_{k=1}^{\infty} R_k(r)\cos k\alpha, \quad (9)$$

$$B_\alpha = -\sum_{k=1}^{\infty} R_k(r)\sin k\alpha. \quad (10)$$

Substituting the assumed solution into expression (7) for the divergence yields:

$$\pm\frac{1}{r}\frac{\partial\left(r\sum_{k=1}^{\infty} R_k(r)\cos k\alpha\right)}{\partial r} - \frac{1}{r}\frac{\partial\left(\sum_{k=1}^{\infty} R_k(r)\sin k\alpha\right)}{\partial\alpha} =$$
$$= \pm\frac{1}{r}\sum_{k=1}^{\infty} R_k(r)\cos k\alpha \pm \sum_{k=1}^{\infty}\frac{\partial R_k(r)}{\partial r}\cos k\alpha -$$
$$-\frac{1}{r}\sum_{k=1}^{\infty} R_k(r)k\cos k\alpha =$$
$$= \pm\sum_{k=1}^{\infty}\left(\frac{\partial R_k(r)}{\partial r} \mp \frac{1}{r}(k\mp 1)R_k(r)\right)\cos k\alpha. \quad (11)$$

Substituting the assumed solution into expression (8) for the rotor yields:

$$-\frac{1}{r}\frac{\partial\left(r\sum_{k=1}^{\infty} R_k(r)\sin k\alpha\right)}{\partial r} \mp \frac{1}{r}\frac{\partial\left(\sum_{k=1}^{\infty} R_k(r)\cos k\alpha\right)}{\partial\alpha} =$$
$$= -\frac{1}{r}\sum_{k=1}^{\infty} R_k(r)\sin k\alpha - \sum_{k=1}^{\infty}\frac{\partial R_k(r)}{\partial r}\sin k\alpha \pm$$
$$\pm\frac{1}{r}\sum_{k=1}^{\infty} R_k(r)k\sin k\alpha =$$
$$= -\sum_{k=1}^{\infty}\left(\frac{\partial R_k(r)}{\partial r} \mp \frac{1}{r}(k\mp 1)R_k(r)\right)\sin k\alpha. \quad (12)$$

In each k-th term of the series of expression (11), and in each k-th term of the series of expression (12), the same factor $\partial R_k(r)/\partial r \mp 1/r(k\mp 1)R_k(r)$ dependent only on r is present, which indicates the success of the application of the method of separation of variables and the correctness of the choice of the type of solution for the variable α.

Equations (7) and (8), taking into account expressions (11) and (12), must be satisfied for any value of α, for which it is necessary and sufficient that the above factor in each k-th term of the series be equal to zero:

$$\frac{\partial R_k(r)}{\partial r} \mp \frac{1}{r}(k\mp 1)R_k(r) = 0. \quad (13)$$

Equation (13) is a linear equation without a right-hand side, the solution of which has the form [14]:

$$R_k(r) = Ce^{\pm\int\frac{k\mp 1}{r}dr} = Ce^{\pm\ln r^{(k\mp 1)}} = Cr^{\pm(k\mp 1)}, \quad (14)$$

where C – an arbitrary constant, the value and dimension of which determine the conditions of a specific problem.

On the surface of the bore of the outer inductor and the turning of the inner inductor, as can be seen from the comparison of (3), (6) with (9), (10), (14):

$$R_k(r_0) = Cr_0^{\pm(k\mp 1)} = \frac{4\rho}{\pi} B_h k_{\beta k} k_{\rho k}, \quad (15)$$

where

$$C = \frac{4\rho}{\pi} B_h k_{\beta k} k_{\rho k} / r_0^{\pm(k\mp 1)}, \quad (16)$$

and, returning to (14):

$$R_k(r) = \frac{4\rho}{\pi} B_h k_{\beta k} k_{\rho k}\left(\frac{r}{r_0}\right)^{\pm(k\mp 1)}. \quad (17)$$

The physical meaning of the solution indicates that:
– the variant based on the "plus" in (6) leads to the relations for the outer inductor:

$$B_r = \frac{4\rho}{\pi} B_h \sum_{k=1}^{\infty}\left(\frac{r}{r_0}\right)^{k-1} k_{\beta k} k_{\rho k}\cos k\alpha, \quad (18)$$

$$B_\alpha = -\frac{4\rho}{\pi} B_h \sum_{k=1}^{\infty}\left(\frac{r}{r_0}\right)^{k-1} k_{\beta k} k_{\rho k}\sin k\alpha; \quad (19)$$

– the variant based on the "minus" in (6) leads to the relations for the inner inductor:

$$B_r = -\frac{4\rho}{\pi} B_h \sum_{k=1}^{\infty}\left(\frac{r_0}{r}\right)^{k+1} k_{\beta k} k_{\rho k}\cos k\alpha, \quad (20)$$

$$B_\alpha = -\frac{4\rho}{\pi} B_h \sum_{k=1}^{\infty}\left(\frac{r_0}{r}\right)^{k+1} k_{\beta k} k_{\rho k}\sin k\alpha. \quad (21)$$

3.2. Magnetic field created by a coil group. The magnetic field induction from the current of a coil group consisting of q identical coils fed by the same current, laid with a constant offset of adjacent coils by an angle $2\theta/p$ (the step along

the coil laying slots), is formed by adding the induction values from individual coils:

$$B_r = \pm\frac{4\rho}{\pi}B_h\sum_{k=1}^{\infty}\left(\frac{r}{r_0}\right)^{\pm(k\mp1)}k_{\beta k}k_{\rho k}\sum_{c=0}^{q-1}\cos k\left(\alpha+c\frac{2\theta}{p}\right), \quad (22)$$

$$B_\alpha = -\frac{4\rho}{\pi}B_h\sum_{k=1}^{\infty}\left(\frac{r}{r_0}\right)^{\pm(k\mp1)}k_{\beta k}k_{\rho k}\sum_{c=0}^{q-1}\sin k\left(\alpha+c\frac{2\theta}{p}\right). \quad (23)$$

The starting point α is along the axis of the outermost coil in the group.

Using the formulas ready for this case [15]:

$$\sum_{k=0}^{n-1}\sin(x+ky)=\sin\left(x+\frac{n-1}{2}y\right)\sin\frac{ny}{2}\operatorname{cosec}\frac{y}{2}, \quad (24)$$

$$\sum_{k=0}^{n-1}\cos(x+ky)=\cos\left(x+\frac{n-1}{2}y\right)\sin\frac{ny}{2}\operatorname{cosec}\frac{y}{2}, \quad (25)$$

and taking into account that there are correspondences between the designations in these formulas and in formulas (22), (23): $k=c$, $n=q$, $x=k\alpha$, $y=k(2\theta/p)$, it is possible to obtain:

$$B_r = \pm\frac{4\rho}{\pi}B_h\sum_{k=1}^{\infty}\left(\frac{r}{r_0}\right)^{\pm(k\mp1)}\times$$

$$\times k_{\beta k}k_{\rho k}\cos k\left(\alpha+\frac{q-1}{2}\frac{2\theta}{p}\right)\sin\frac{kq\dfrac{2\theta}{p}}{2}/\sin k\frac{\dfrac{2\theta}{p}}{2}=$$

$$=\pm\frac{4q\rho}{\pi}B_h\sum_{k=1}^{\infty}\left(\frac{r}{r_0}\right)^{\pm(k\mp1)}k_{wk}\cos k\left(\alpha+(q-1)\frac{\theta}{p}\right), \quad (26)$$

$$B_\alpha = -\frac{4\rho}{\pi}B_h\sum_{k=1}^{\infty}\left(\frac{r}{r_0}\right)^{\pm(k\mp1)}\times$$

$$\times k_{\beta k}k_{\rho k}\sin k\left(\alpha+\frac{q-1}{2}\frac{2\theta}{p}\right)\sin\frac{kq\dfrac{2\theta}{p}}{2}/\sin k\frac{\dfrac{2\theta}{p}}{2}=$$

$$=-\frac{4q\rho}{\pi}B_h\sum_{k=1}^{\infty}\left(\frac{r}{r_0}\right)^{\pm(k\mp1)}k_{wk}\sin k\left(\alpha+(q-1)\frac{\theta}{p}\right), \quad (27)$$

where $k_{wk}=k_{\rho k}k_{\beta k}k_{\theta k}$ – the winding coefficient of the coil group.

$$k_{\theta k}=\frac{\sin k\dfrac{q\theta}{p}}{q\sin k\dfrac{\theta}{p}}, \quad (28)$$

where $k_{\theta k}$ – the distribution coefficient of the coil group of the k-th member of the series, θ – the half of the shift angle between adjacent coils multiplied by p.

Let's shift the origin of the coordinate α by an angle $(q-1)(\theta/p)$, that is, by the axis of the coil group, and obtain the expansion in a Fourier series of the components of the induction vector from the current of the *coil group* in the following form:

$$B_r = \pm\frac{4q\rho}{\pi}B_h\sum_{k=1}^{\infty}\left(\frac{r}{r_0}\right)^{\pm(k\mp1)}k_{wk}\cos k\alpha, \quad (29)$$

$$B_\alpha = -\frac{4q\rho}{\pi}B_h\sum_{k=1}^{\infty}\left(\frac{r}{r_0}\right)^{\pm(k\mp1)}k_{wk}\sin k\alpha. \quad (30)$$

3.3. Magnetic field of the phase. The symmetrical windings typical of electric machines, which induce a magnetic field without even harmonics, are considered. In particular, these include all types of diametrical windings, in which the shortening factor $k_{\beta k}$ is zero for even harmonics. The important case of an even number n of coil groups with the same shortened pitch with pairwise matching connection (each pair of adjacent coil groups forms two magnetic poles $p=n/2$) is considered separately.

Let's add up the components of the magnetic induction vector from the currents of an even number of identical coil groups of a *single-phase circuit* of a symmetrical winding of an inductor, connected pairwise matching:

$$B_r = \pm\frac{4q\rho}{\pi}B_h\sum_{k=1}^{\infty}\left(\frac{r}{r_0}\right)^{\pm(k\mp1)}k_{wk}\sum_{j=0}^{n-1}(-1)^j\cos k\left(\alpha+j\frac{2\pi}{n}\right), \quad (31)$$

$$B_\alpha = -\frac{4q\rho}{\pi}B_h\sum_{k=1}^{\infty}\left(\frac{r}{r_0}\right)^{\pm(k\mp1)}k_{wk}\sum_{j=0}^{n-1}(-1)^j\sin k\left(\alpha+j\frac{2\pi}{n}\right). \quad (32)$$

Summation over j yields zero for all $k\neq(n/2)\nu$, where $\nu=1, 3, 5, \ldots$ – an odd number, therefore:

$$B_r = \pm\frac{4qn\rho}{\pi}B_h\sum_{\nu=1,3,5\ldots}^{\infty}\left(\frac{r}{r_0}\right)^{\pm\left(\frac{n}{2}\nu\mp1\right)}k_{w\nu}\times$$

$$\times\sum_{j=0}^{n-1}(-1)^j\cos\left(\frac{n}{2}\nu\alpha+j\pi\right), \quad (33)$$

$$B_\alpha = -\frac{4qn\rho}{\pi}B_h\sum_{\nu=1,3,5\ldots}^{\infty}\left(\frac{r}{r_0}\right)^{\pm\left(\frac{n}{2}\nu\mp1\right)}k_{w\nu}\times$$

$$\times\sum_{j=0}^{n-1}(-1)^j\sin\left(\frac{n}{2}\nu\alpha+j\pi\right), \quad (34)$$

or

$$B_r = \pm\frac{4W\rho}{\pi w}B_h\sum_{\nu=1,3,5\ldots}^{\infty}\left(\frac{r}{r_0}\right)^{\pm(p\nu\mp1)}k_{w\nu}\cos p\nu\alpha, \quad (35)$$

$$B_\alpha = -\frac{4W\rho}{\pi w}B_h\sum_{\nu=1,3,5\ldots}^{\infty}\left(\frac{r}{r_0}\right)^{\pm(p\nu\mp1)}k_{w\nu}\sin p\nu\alpha, \quad (36)$$

where p – the number of pole pairs of the magnetic field created by the currents of the single-phase circuit of the inductor winding, $p=n/2$; W – the number of turns of the phase winding, $W=qnw$.

Thus, in the case of harmonious inclusion, there are no even harmonics in the inductor field.

Inductor winding coefficient:

$$k_{w\nu}=k_{\rho\nu}k_{\beta\nu}k_{\theta\nu}=\frac{\sin p\nu\rho}{p\nu\rho}\cdot\sin\left(\nu\beta\frac{\pi}{2}\right)\cdot\frac{\sin\nu q\theta}{q\sin\nu\theta}, \quad (37)$$

where $k_{\beta\nu}=\sin\left(\nu\beta\dfrac{\pi}{2}\right)$ – the winding shortening coefficient, known in the general theory of electrical machines, $k_{\theta\nu}=\dfrac{\sin\nu q\theta}{q\sin\nu\theta}$ – the winding distribution coefficient, known in the general theory of electrical machines.

ISSN 2664-9969

Formulas (35)–(37) are further accepted for use with any symmetrical windings that ensure the absence of even harmonics and for which the parameters $W, p, q, \rho, \beta, \theta$ are defined.

3.4. Magnetic field of the *m*-phase winding. *The rotating magnetic field* in the inductor, represented by the components of the magnetic induction vector, is formed by adding the components of the field induction vectors from sinusoidal in time t (s) with frequency ω (s^{-1}) currents of m single-phase circuits with a phase shift step from circuit to circuit $\Delta\omega t = 2\pi/m$ with a sequential shift of the circuit axes with a step $\Delta\alpha = 2\pi/mp$.

In this case, (1) is taken into account in the form:

$$B_h = \mu_0 \frac{I_m w}{2\rho r_0}, \tag{38}$$

where I_m – the amplitude value of the current in a single-phase circuit.

Let's agree to understand by the designation $B_{n\nu}$:

$$B_{n\nu} = \begin{cases} \dfrac{4W\rho}{\pi w} B_h \left(\dfrac{r}{r_0}\right)^{p\nu-1} k_{w\nu}, \\ \dfrac{4W\rho}{\pi w} B_h \left(\dfrac{r}{r_0}\right)^{-(p\nu+1)} k_{w\nu}. \end{cases} \tag{39}$$

Then in the m-phase inductor:

$$B_r = \pm\sum_{\nu=1,3,5\ldots} B_{n\nu} \times \times\sum_{\sigma=0}^{m-1}\cos\left(\omega t-\sigma\frac{2\pi}{m}\right)\cos p\nu\left(\alpha-\sigma\frac{2\pi}{mp}\right)= = \pm\sum_{\nu=1,3,5\ldots} B_{n\nu} \times \times\sum_{\sigma=0}^{m-1}\cos\left(\omega t-\sigma\frac{2\pi}{m}\right)\cos\left(p\nu\alpha-\nu\sigma\frac{2\pi}{m}\right), \tag{40}$$

$$B_\alpha = \sum_{\nu=1,3,5\ldots}^{\infty} B_{n\nu} \times \times\sum_{\sigma=0}^{m-1}\cos\left(\omega t-\sigma\frac{2\pi}{m}\right)\sin p\nu\left(\alpha+\sigma\frac{2\pi}{mp}\right)= = \sum_{\nu=1,3,5\ldots}^{\infty} B_{n\nu} \times \times\sum_{\sigma=0}^{m-1}\cos\left(\omega t-\sigma\frac{2\pi}{m}\right)\sin\left(p\nu\alpha+\nu\sigma\frac{2\pi}{m}\right). \tag{41}$$

If the harmonic number ν is a multiple of m, then:

$$\sum_{\sigma=0}^{m-1}\cos\left(\omega t-\sigma\frac{2\pi}{m}\right)\cos\left(p\nu\alpha-\nu\sigma\frac{2\pi}{m}\right)= = \cos(p\nu\alpha)\sum_{\sigma=0}^{m-1}\cos\left(\omega t-\sigma\frac{2\pi}{m}\right)=0, \tag{42}$$

$$\sum_{\sigma=0}^{m-1}\cos\left(\omega t-\sigma\frac{2\pi}{m}\right)\sin\left(p\nu\alpha-\nu\sigma\frac{2\pi}{m}\right)= = \sin(p\nu\alpha)\sum_{\sigma=0}^{m-1}\cos\left(\omega t-\sigma\frac{2\pi}{m}\right)=0, \tag{43}$$

from which it follows (taking into account the absence of even harmonics) that in the field of the m-phase inductor there are those harmonics of the field whose numbers ν satisfy the following expressions:

$$\nu = \begin{cases} 2me+1, & e=0,1,2,3\ldots\infty, \\ 2ms-1, & s=1,2,3\ldots\infty. \end{cases} \tag{44}$$

Then,

$$B_r = \pm\sum_{\nu=2me+1} B_{n\nu}\sum_{\sigma=0}^{m-1}\cos\left(\omega t-\sigma\frac{2\pi}{m}\right)\cos\left(p\nu\alpha-\nu\sigma\frac{2\pi}{m}\right)\pm \pm\sum_{\nu=2ms-1} B_{n\nu}\sum_{\sigma=0}^{m-1}\cos\left(\omega t-\sigma\frac{2\pi}{m}\right)\cos\left(p\nu\alpha-\nu\sigma\frac{2\pi}{m}\right)= = \pm\sum_{\nu=2me+1} B_{n\nu}\sum_{\sigma=0}^{m-1}\cos\left(\omega t-\sigma\frac{2\pi}{m}\right)\cos\left(p\nu\alpha-(2me+1)\sigma\frac{2\pi}{m}\right)\pm \pm\sum_{\nu=2ms-1} B_{n\nu}\sum_{\sigma=0}^{m-1}\cos\left(\omega t-\sigma\frac{2\pi}{m}\right)\cos\left(p\nu\alpha-(2ms-1)\sigma\frac{2\pi}{m}\right)= = \pm\sum_{\nu=2me+1} B_{n\nu}\sum_{\sigma=0}^{m-1}\cos\left(\omega t-\sigma\frac{2\pi}{m}\right)\cos\left(p\nu\alpha-\sigma\frac{2\pi}{m}\right)\pm \pm\sum_{\nu=2ms-1} B_{n\nu}\sum_{\sigma=0}^{m-1}\cos\left(\omega t-\sigma\frac{2\pi}{m}\right)\cos\left(p\nu\alpha+\sigma\frac{2\pi}{m}\right)= = \pm0.5\sum_{\nu=2me+1} B_{n\nu}\sum_{\sigma=0}^{m-1}\left(\cos(\omega t-p\nu\alpha)+\cos\left(\omega t+p\nu\alpha-2\sigma\frac{2\pi}{m}\right)\right)\pm \pm0.5\sum_{\nu=2ms-1} B_{n\nu}\sum_{\sigma=0}^{m-1}\left(\cos\left(\omega t-p\nu\alpha-2\sigma\frac{2\pi}{m}\right)+\cos(\omega t+p\nu\alpha)\right)= = \pm0.5\sum_{\nu=2me+1} B_{n\nu}\sum_{\sigma=0}^{m-1}\left(\cos(\omega t-p\nu\alpha)+\cos(\omega t+p\nu\alpha)\cos2\sigma+ +\sin(\omega t+p\nu\alpha)\sin2\sigma\frac{2\pi}{m}\right)\pm0.5\sum_{\nu=2ms-1}\times \times B_{n\nu}\sum_{\sigma=0}^{m-1}\left(\cos(\omega t-p\nu\alpha)\cos2\sigma\frac{2\pi}{m}+ +\sin(\omega t-p\nu\alpha)\sin2\sigma\frac{2\pi}{m}+\cos(\omega t+p\nu\alpha)\right)= = \pm0.5m\sum_{\nu=2me+1} B_{n\nu}\cos(\omega t-p\nu\alpha)\pm \pm0.5m\sum_{\nu=2ms-1} B_{n\nu}\cos(\omega t+p\nu\alpha); \tag{45}$$

$$B_\alpha = -\sum_{\nu=2me+1} B_{n\nu}\sum_{\sigma=0}^{m-1}\cos\left(\omega t-\sigma\frac{2\pi}{m}\right)\sin\left(p\nu\alpha-\nu\sigma\frac{2\pi}{m}\right)- -\sum_{\nu=2ms-1} B_{n\nu}\sum_{\sigma=0}^{m-1}\cos\left(\omega t-\sigma\frac{2\pi}{m}\right)\sin\left(p\nu\alpha-\nu\sigma\frac{2\pi}{m}\right)= = -\sum_{\nu=2me+1} B_{n\nu}\sum_{\sigma=0}^{m-1}\cos\left(\omega t-\sigma\frac{2\pi}{m}\right)\sin\left(p\nu\alpha-(2me+1)\sigma\frac{2\pi}{m}\right)- -\sum_{\nu=2ms-1} B_{n\nu}\sum_{\sigma=0}^{m-1}\cos\left(\omega t-\sigma\frac{2\pi}{m}\right)\sin\left(p\nu\alpha-(2ms-1)\sigma\frac{2\pi}{m}\right)= = -\sum_{\nu=2me+1} B_{n\nu}\sum_{\sigma=0}^{m-1}\cos\left(\omega t-\sigma\frac{2\pi}{m}\right)\sin\left(p\nu\alpha-\sigma\frac{2\pi}{m}\right)- -\sum_{\nu=2ms-1} B_{n\nu}\sum_{\sigma=0}^{m-1}\cos\left(\omega t-\sigma\frac{2\pi}{m}\right)\sin\left(p\nu\alpha+\sigma\frac{2\pi}{m}\right)= = -0.5\sum_{\nu=2me+1} B_{n\nu}\sum_{\sigma=0}^{m-1}\left(\sin\left(\omega t+p\nu\alpha-2\sigma\frac{2\pi}{m}\right)-\sin(\omega t-p\nu\alpha)\right)- -0.5\sum_{\nu=2ms-1} B_{n\nu}\sum_{\sigma=0}^{m-1}\left(\sin(\omega t+p\nu\alpha)-\sin\left(\omega t-p\nu\alpha-2\sigma\frac{2\pi}{m}\right)\right)= = -0.5\sum_{\nu=2me+1} B_{n\nu}\sum_{\sigma=0}^{m-1}\left(\sin(\omega t+p\nu\alpha)\cos2\sigma\frac{2\pi}{m}+ +\cos(\omega t+p\nu\alpha)\sin2\sigma\frac{2\pi}{m}-\sin(\omega t-p\nu\alpha)\right)- -0.5\sum_{\nu=2ms-1} B_{n\nu}\sum_{\sigma=0}^{m-1}\left(\sin(\omega t+p\nu\alpha)-\sin(\omega t-p\nu\alpha)\cos2\sigma\frac{2\pi}{m}\right)+ +\cos\left((\omega t-p\nu\alpha)\sin2\sigma\frac{2\pi}{m}\right)=0.5m\sum_{\nu=2me+1} B_{n\nu}\sin(\omega t-p\nu\alpha)- -0.5m\sum_{\nu=2ms-1} B_{n\nu}\sin(\omega t+p\nu\alpha). \tag{46}$$

It was taken into account that:

$$\sum_{\sigma=0}^{m-1}\sin 2\sigma\frac{2\pi}{m}=\sum_{\sigma=0}^{m-1}\cos 2\sigma\frac{2\pi}{m}=0.$$

3.5. Generalized formulas for analytical calculations of the magnetic field in reactors with cylindrical inductors. Taking into account (38), (39), (45), (46) let's obtain the desired generalized formulas for calculating and analyzing the magnetic field in a reactor, which relate the components of the induction vector of a plane-parallel elliptical magnetic field of an m-phase inductor to the parameters of the latter.

For an external inductor:

$$B_r=\mu_0\frac{I_m W}{r_0}\cdot\frac{m}{\pi}\sum_{\nu=2me+1}\left(\frac{r}{r_0}\right)^{p\nu-1}k_{\omega\nu}\cos(\omega t-p\nu\alpha)+$$

$$+\mu_0\frac{I_m W}{r_0}\cdot\frac{m}{\pi}\sum_{\nu=2ms-1}\left(\frac{r}{r_0}\right)^{p\nu-1}k_{\omega\nu}\cos(\omega t+p\nu\alpha), \qquad (47)$$

$$B_\alpha=\mu_0\frac{I_m W}{r_0}\cdot\frac{m}{\pi}\sum_{\nu=2me+1}\left(\frac{r}{r_0}\right)^{p\nu-1}k_{\omega\nu}\sin(\omega t-p\nu\alpha)-$$

$$-\mu_0\frac{I_m W}{r_0}\cdot\frac{m}{\pi}\sum_{\nu=2ms-1}\left(\frac{r}{r_0}\right)^{p\nu-1}k_{\omega\nu}\sin(\omega t+p\nu\alpha). \qquad (48)$$

For an internal inductor:

$$B_r=-\mu_0\frac{I_m W}{r_0}\cdot\frac{m}{\pi}\sum_{\nu=2me+1}\left(\frac{r}{r_0}\right)^{-(p\nu+1)}k_{\omega\nu}\cos(\omega t-p\nu\alpha)-$$

$$-\mu_0\frac{I_m W}{r_0}\cdot\frac{m}{\pi}\sum_{\nu=2ms-1}\left(\frac{r}{r_0}\right)^{-(p\nu+1)}k_{\omega\nu}\cos(\omega t+p\nu\alpha), \qquad (49)$$

$$B_\alpha=\mu_0\frac{I_m W}{r_0}\cdot\frac{m}{\pi}\sum_{\nu=2me+1}\left(\frac{r}{r_0}\right)^{-(p\nu+1)}k_{\omega\nu}\sin(\omega t-p\nu\alpha)-$$

$$-\mu_0\frac{I_m W}{r_0}\cdot\frac{m}{\pi}\sum_{\nu=2ms-1}\left(\frac{r}{r_0}\right)^{-(p\nu+1)}k_{\omega\nu}\sin(\omega t+p\nu\alpha). \qquad (50)$$

Here B_r, B_α – the scalar components of the magnetic field induction vector $\vec{B}$ at a point in the working zone of the inductor, T; m – the number of phases; ν – the harmonic number; $e=0, 1, 2, 3, ..., \infty$; $s=1, 2, 3, ..., \infty$; $\mu_0=4\pi\cdot10^{-7}$ H/m is the magnetic constant; I_m – the peak value of the phase current, A; W – the number of turns in the phase; p – the number of pole pairs of the fundamental harmonic; $k_{\omega\nu}=k_{p\nu}k_{\theta\nu}k_{\beta\nu}$ – the winding coefficient for the ν-th harmonic component; $k_{p\nu}=\frac{\sin p\nu\rho}{p\nu\rho}$ – the slot opening coefficient, ρ – the half of the slot opening angle; $k_{\beta\nu}=\sin\nu\beta\frac{\pi}{2}$ – the shortening factor (β – the relative winding pitch); $k_{\theta\nu}=\frac{\sin\nu q\theta}{q\sin\nu\theta}$ – the winding distribution coefficient (θ – the half of the displacement angle of adjacent coils of the coil group multiplied by p, rad), q – the number of coils in the coil group, at $q=1$ ($\theta=0$) the coefficient is $k_{\theta\nu}=1$; r in meters and α in radians are the polar coordinates with the pole on the inductor axis (α is measured from the axis of the phase in which the current reaches the peak value at the moment the time count begins); r_0 – the radius of the bore of the outer or turning of the inner inductor, m; ω – the angular frequency, s^{-1} ($\omega=2\pi f$, where f – the frequency of the power supply voltage, Hz); t – time, s.

3.6. Explanations for formulas (47)–(50). The induction vector of each field harmonic is described by the formulas of a circular field (i. e. the hodograph of the rotating induction vector of any harmonic is a circle) and rotates at a constant speed ω [10]. For the external inductor, the group of forward-rotating harmonics with numbers $\nu=2me+1$, $e=0, 1, 2, ..., \infty$ rotates in the direction of the coordinate α, the group of backward-rotating harmonics $\nu=2ms-1$, $s=1, 2, 3, ..., \infty$ rotates in the opposite direction. For the internal inductor, the directions of rotation of the induction vectors of the harmonics of the specified groups change to the opposite ones. The direction of the vector $\vec{B}_\nu$ of each harmonic does not depend on the coordinate r, and the modulus B_ν does not depend on the coordinate α:

$$B_\nu=B_{0\nu}\left(\frac{r}{r_0}\right)^{\pm(p\nu\mp1)}, \qquad (51)$$

where $B_{0\nu}=\mu_0\frac{I_m W}{r_0}\cdot\frac{m}{\pi}\cdot k_{\omega\nu}$.

Dependence (51) of the modulus of the fundamental harmonic of the induction of the reactor RMF on the relative radius for external and internal inductors with a different number of pole pairs is shown graphically in Fig. 2. For the external inductor $r/r_0\le1$; for the internal inductor $r/r_0\ge1$. The value of the modulus of the first harmonic of the induction on the boundary circle of radius r_0 is taken to be the same for all cases and is taken as 1.

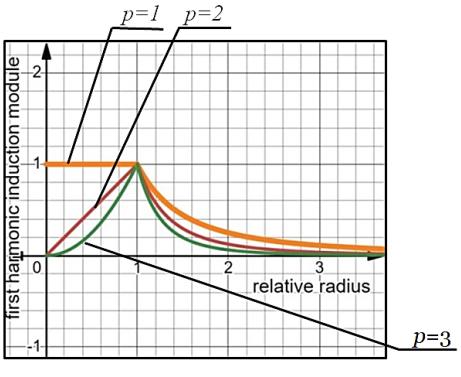

Fig. 2. Dependence of the first harmonic of the RMF magnetic induction vector MF in the cross-section of the inductor working space on the relative radius r/r_0 in inductors with different numbers of pole pairs p

The sum of the magnetic induction vectors of the forward-rotating harmonics is a certain vector $\vec{B}^+$ that is constant in modulus and rotates with a constant speed ω. The resulting vector $\vec{B}^-$ of the counter-rotating harmonics is constant in modulus and rotates in the opposite direction with the same angular velocity. Thus, the induction vector $\vec{B}$ is the sum of two vectors and that are constant in modulus $\vec{B}^+$ and $\vec{B}^-$ rotate in different directions with the same angular velocity and have moduli B^+ and B^-. From this, as is known [16], it follows that the hodograph of the induction vector of magnetic field is an ellipse with semi-axes:

$$B_{\min}=B^+-B^- \text{ and } B_{\max}=B^++B^-.$$

Thus, according to the nature of rotation of the magnetic induction vector, the considered RMF is elliptical. The vector $\vec{B}$ at any point in the working space of the reactor rotates in

ISSN 2664-9969

the same direction as the vector of the first harmonic, or vector $\vec{B}^+$, and makes a complete revolution, returning to the initial position on the hodograph, in the same time as the vectors $\vec{B}^+$ and $\vec{B}^-$. The instantaneous angular velocity of the vector $\vec{B}$ is not constant, but changes with a period of half a revolution of this vector. The expression for the instantaneous angular velocity ω' of the vector $\vec{B}$ is given in an early work [11] without a derivation. Let's give a derivation: taking the time derivative of the angle ϑ between the vector $\vec{B}$ and the long semi-axis of the ellipse, while assuming that $t=0$, when $B=B_{\max}$:

$$\omega' = d\vartheta/dt = d\left(\operatorname{arctg}\frac{B_{\min}\sin(\omega t)}{B_{\max}\cos(\omega t)}\right)/dt =$$

$$= d\left(\operatorname{arctg}\left(\frac{B_{\min}}{B_{\max}}\operatorname{tg}\omega t\right)\right)/dt =$$

$$= \frac{\frac{B_{\min}}{B_{\max}}}{1+\left(\frac{B_{\min}}{B_{\max}}\operatorname{tg}\omega t\right)^2}\cdot\frac{\omega}{\cos^2\omega t} = \frac{\frac{B_{\min}}{B_{\max}}\omega}{\cos^2\omega t+\left(\frac{B_{\min}}{B_{\max}}\right)^2\sin^2\omega t}.$$

Let's obtain the final formula:

$$\omega' = \frac{\frac{B_{\min}}{B_{\max}}\omega}{\cos^2\omega t+\left(\frac{B_{\min}}{B_{\max}}\right)^2\sin^2\omega t}, \qquad (52)$$

which provides a tool for calculating the relative (ω'/ω) instantaneous angular velocity of the rotating vector of magnetic induction of elliptical RMF of the class under consideration and will be used below (*example No. 1*).

As follows from formulas (47)–(52), the effect of higher harmonics of induction on the RMF characteristics with distance from the surface of the inductor core with distributed longitudinal currents decreases the more, the greater the harmonic number. Therefore, the characteristics of the magnetic field in the working areas of the reactor remote from the specified surface of the core approach the characteristics of the circular field of the first harmonic. The RMF of the first harmonic in a reactor with a two-pole external inductor is a circular uniform rotating vector field. In all other cases, the magnetic field of the first harmonic is a circular non-uniform rotating vector field. Near the core surface, the resulting magnetic induction vector in the reactor in all the studied cases rotates along a clearly defined elliptical hodograph, which, as will be shown below, has a different tilt angle, different absolute values and axis ratios, and a certain spatial periodicity for different operating points.

The force action of the RMF with elliptical inhomogeneity on the MP differs significantly from the force action of the circular magnetic field considered in [10]. Consideration of the issues of the force action of the elliptical RMF of reactors on the MP and the processed medium is beyond the scope of this work.

The emergence of new formulas is always accompanied by a lot of work to confirm them and clarify the details of the area of application. Since formulas (47)–(52) cover a significant range of different types (number of pole pairs) and designs (stator, stationary rotor) of cylindrical inductors, it is impossible to provide examples of confirmation of their adequacy for each type and design of reactors in one article. In this paper, let's limit ourselves to examples of calculating the RMF characteristics of several reactors using exclusively external two-pole inductors. Such reactors are most widely used in practice. The working chamber of the reactor is a pipe or vessel inserted into the bore of the external inductor with the number of pole pairs of the winding $p=1$. This pipe or vessel is filled with the processed medium and working magnetic particles. An important geometric parameter of the reactor, affecting the content of higher harmonics in its RMF, is the ratio r_i/r_0, where r_i – the inner radius of the working vessel. In industrial applications, the inner radius of the reactor working pipe usually amounts to 0.8–0.95 of the bore radius. In scientific applications of reactors, the task is often set to ensure operation in a field region with a low content of higher harmonics. In these cases, the inner radius of the working vessel, depending on the distribution of the winding and the design of the inductor, as well as on the level of requirements for the field "purity", is selected from the condition $r_i/r_0 < 0.8-0.1$ (see papers [8, 9] and *examples No. 1–3* below). It also follows from the structure of formulas (47)–(52) that a reduction in the level of higher harmonics in the reactor's RMF at a given relative radius can be achieved by methods known from the theory of electrical machines: by distributing the winding with $q>2$, as well as by shortening the step by 0.8–0.86 and increasing the number of phases. The influence of these factors is considered in *examples No. 2 and No. 3* below.

Note. Previously presented formulas with $\nu = 1\pm 6e$ [11]:

$$B_r = \mu_0\frac{I_m w q n}{r_0}\frac{3}{\pi}\sum_{\nu=1\pm 6e}k_{w|\nu|}\left(\frac{r}{r_0}\right)^{p|\nu|-1}\cos(\omega t - p\nu\alpha),$$

$$B_\alpha = \frac{\nu}{|\nu|}\mu_0\frac{I_m w q n}{r_0}\frac{3}{\pi}\sum_{1\pm 6e}k_{w|\nu|}\left(\frac{r}{r_0}\right)^{p|\nu|-1}\sin(\omega t - p\nu\alpha),$$

are limited to the special case of three-phase external inductors and are less convenient for analysis.

3.7. Examples of calculations and analysis of rotating magnetic fields of reactors at idle (without magnetic particles) and their verification. To calculate the RMF characteristics in reactors using formulas (47)–(52) and to plot the necessary graphs, the Desmos graphical calculator was used. For brevity, this calculation method and its results will be denoted by the letters FD. Only the first ten harmonics from the Fourier series of formulas (47)–(50) were taken into account. In this case, the calculation results change insignificantly, and the calculation time is significantly reduced. The FD calculation results were compared with the experiment or literature data containing RMF calculations of similar inductors using various programs using the finite element method.

In *examples No. 1 and No. 3*, the values of B, B_r, B_α are represented by ratios to the modulus of the first harmonic of the field induction vector, the values of ω' are represented by ratios to the angular frequency ω.

In the first example, the results of FD calculations are compared with the results of measurements, in the second and third examples, the results of FD calculations are compared with the results of calculations by numerical field methods.

Example No. 1. A reactor with a simple three-phase external salient-pole inductor for six removable teeth, fastened to the yoke with bolts and embedded bushings (380 V, 50 Hz).

The external inductor of such reactors is usually placed in a protective casing, which includes a thin cylindrical bushing, limiting the bore, and creating space for the circulation of the cooling agent. The inductor has a simple winding connected according to a circuit that ensures the number of pole pairs $p=1$. The inductor section and winding connection circuit are shown in Fig. 3 (the inductor protective casing and the boring sleeve separating the inductor from the reactor working chamber are not shown in Fig. 3). Each phase in this design has two opposite coils (of the same color in the figure). The circles indicate the directions of axial currents in the coils of phase C at one of the moments in time. The axis $\alpha=0$ is the axis of phase A. The calculated parameters of the inductor are $m=3$; $p=1$; $q=1$ ($k_{\theta v}=1$); $\beta=1/3$ (the winding is shortened and connected in pairs according); $\rho=0.05$; $\omega=314$ s^{-1}.

The calculations demonstrate FD graphs of the radial B_r, tangential B_α components and the module B of the resulting induction, since all these RMF characteristics are important in reactors for calculating the torques and forces acting on the MP.

Some FD characteristics of a plane-parallel RMF on representative circles of different relative radii r/r_0 in the bore of such inductors depending on the coordinate α are shown in Fig. 4.

The peak values of the modulus B of the induction on the circle $r/r_0=0.8$ during field rotation (the field rotation is simulated on the calculator by introducing a dynamic slider for the parameter ωt) do not go beyond the limits of 1.88/0.47, indicated in Fig. 4 by dotted lines. On the circle $r/r_0=0.5$ the peak values of induction during the field rotation are equal to 1.08/0.92 (i. e. the maximum deviations of the resulting magnetic induction modulus from the first harmonic modulus are ±8 %).

The induction vector hodographs for a given inductor under any slot at the same relative radius are the same. The hodographs under the teeth are also repeated at a step of $\pi/3$ along the α coordinate.

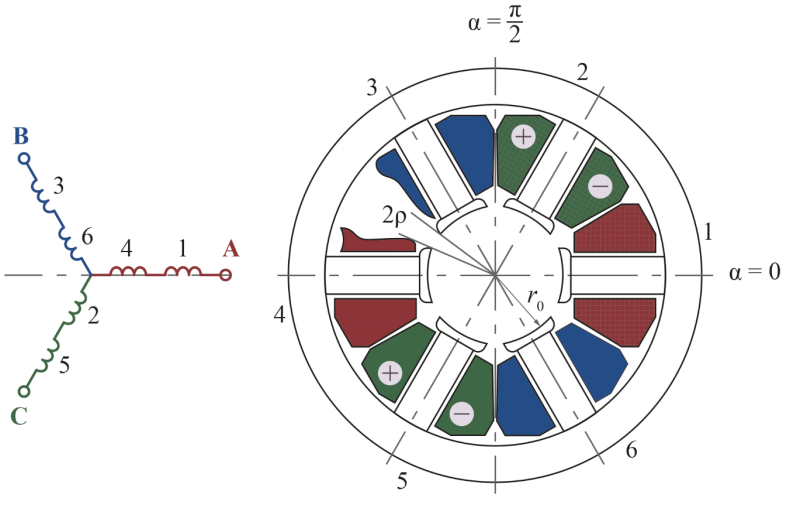

Fig. 3. Cross-section and connection diagram of a two-pole three-phase external inductor with six slots and a symmetrical winding containing six identical coils with a shortened pitch

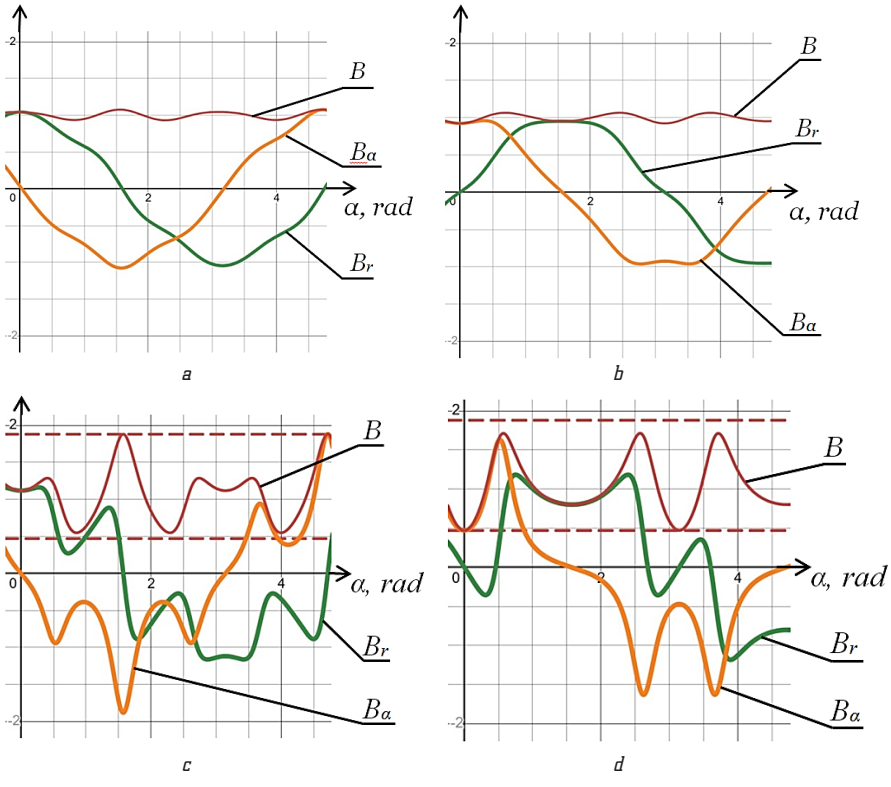

Fig. 4. Dependence on the coordinate α: radial B_r, tangential B_α components and the modulus B of the magnetic induction vector in the inductor bore on representative circles of different relative radii for two moments in time: *a* – $r/r_0=0.5$, $\omega t=0$; *b* – $r/r_0=0.5$, $\omega t=\pi/2$; *c* – $r/r_0=0.8$, $\omega t=0$; *d* – $r/r_0=0.8$, $\omega t=\pi/2$

ISSN 2664-9969

In other words, the distribution of hodographs along the α coordinate has a spatial periodicity with a period of π/3. The full FD characteristics of the RMF behavior depending on time at two boring points (along the slot axis and along the tooth axis) close to the tooth-slot surface are shown in Fig. 5, 6. The induction components are harmonic in nature. At the presented points, their phase shift is equal to π/2, which indicates the location of the hodograph axes along the coordinate axes. At other points, the phase shift between the induction components is not equal to π/2, as a result, the hodograph axes do not coincide with the coordinate axes and the hodograph acquires an inclined character.

As can be seen from Fig. 5, 6, the speed and module of the rotating resulting induction vector retain periodicity, but their instantaneous values at the reactor operating points close to the core surface $r=r_0$ can vary within wide limits. In practice, this causes significant changes in the force effect of the RMF and the behavior of MPs in various working zones of the reactor (central region, periphery, wall zones).

Experimental confirmation of the calculations was obtained on two types of inductors:

1) an inductor with a bore diameter of 100 mm and an induction at the center of 0.12 T;

2) an inductor with a bore diameter of 150 mm and an induction at the center of 0.15 T.

The values of the induction components were measured at several characteristic points of the bore. The measurements were carried out in the standard mode of the inductor at idle (in the absence of MP) using a miniature induction sensor. At some points, the phase shift, the change in the induction components over time, the orientation and type of hodographs were studied. For this purpose, a special two-coordinate induction sensor was made, which is two flat circular calibrated microcoils with a common center, located in mutually perpendicular planes. The discrepancies between the calculated and experimental data in all cases were commensurate with the measurement error and did not exceed several percent.

Typical results of measurements of the values of the induction components (for an inductor with a bore diameter of 100 mm) are presented in Table 1 (B_c is the induction module in the bore center).

Note on the non-standard manufacture of a salient-pole inductor. A three-phase inductor with six coils mounted on removable teeth and a slot opening at an angle of $2\rho = 0.1 \div 0.2$ rad is a widely used standard design for implementing a uniform circular RMF of the first harmonic of magnetic induction in reactors [1–3, 5, 8, 10, 11, 17].

The advantages of this inductor are its simple manufacturing and repair technology, as well as the short length of the winding end parts, which reduces the weight and length of the reactor working chamber (necessary in technologies with frequent removal and installation of the chamber). When calculating the RMF of such an inductor, a relative winding pitch of β=1/3 is used. According to the first developers of this inductor [17], with a further increase in the slot opening, the shortening factor decreases significantly (since the coil turns are not distributed uniformly over the slot, but are concentrated in one of the slot halves near the corresponding tooth). And also, the saturation of the teeth increases, and in general the inductor performance deteriorates. It often happens that researchers do not take this into account when independently producing similar designs.

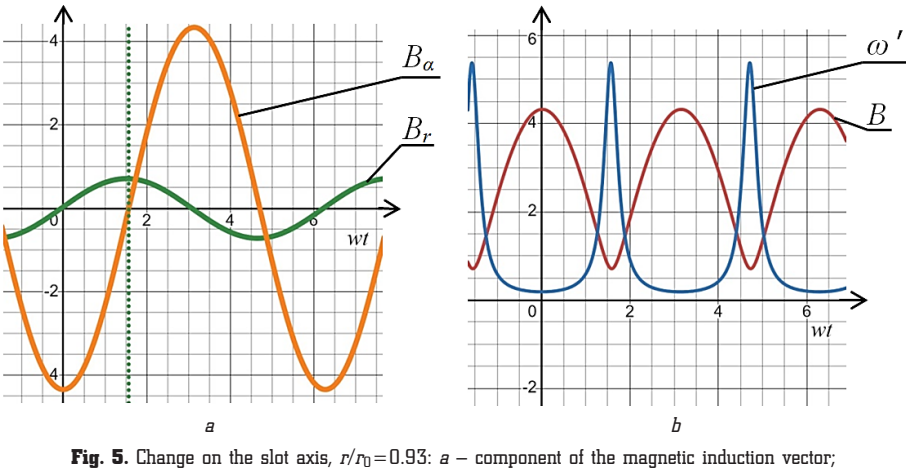

Fig. 5. Change on the slot axis, $r/r_0=0.93$: *a* – component of the magnetic induction vector; *b* – modulus B and angular velocity ω′ of the magnetic induction vector

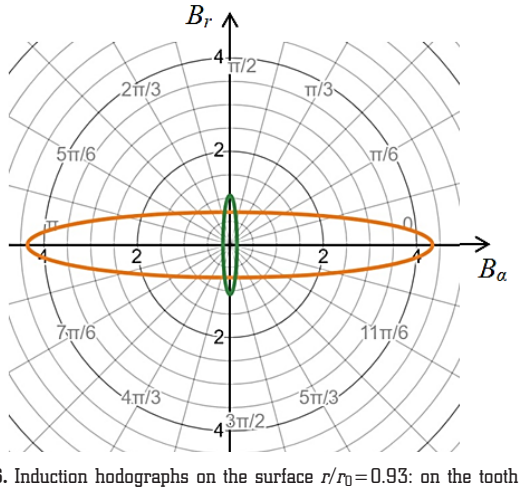

Fig. 6. Induction hodographs on the surface $r/r_0=0.93$: on the tooth axis, a vertically located ellipse and on the slot axis, a horizontally located ellipse

Table 1

Comparison of calculated and experimental values of the induction components in the bore of the inductor

α, rad	r/r_0	Hodograph semi-axes in relative units			
		$B_{r\max}/B_c$		$B_{\alpha\max}/B_c$	
		FD calculation	Measurements	FD calculation	Measurements
Tooth axis	0.5	1.05	1.1	0.92	0.95
	0.7	1.11	1.15	0.68	0.7
	0.8	1.12	1.2	0.47	0.5
	0.9	1.08	1.15	0.23	0.25
Slot axis	0.5	0.952726	0.95	1.078364	1.15
	0.7	0.861868	0.85	1.39756	1.45
	0.8	0.800937	0.8	1.880993	1.9
	0.9	0.734745	0.75	3.302783	3.4

For example, in the work [9], on the creation of a mechatronic reactor for biological applications, to improve the design characteristics for the stated purposes, it is advisable to use removable teeth and reduce the slot opening to the optimal value. At the same time, increasing the cross-section of the teeth to the standard work "on the knee" of the steel magnetization curve. To switch to a diametrical winding pitch while maintaining a small overhang of the frontal parts, it is possible to try Gramme coils, which cover the yoke of the core. In this case, the coils are put on a split yoke of the core between the teeth, or are wound between the teeth on a solid core. If it is necessary to create a reactor for operation in a precision homogeneous RMF, a six-phase Gramme system with 12 slots, described in *example No. 3*, can be used.

Example No. 2. A reactor with a three-phase two-pole external inductor with a distributed winding: bore diameter 350 mm; 380 V; 50 Hz; 0.25 T in the bore center.

A reactor with such an inductor is described in work [2]. The advantage of such an inductor in comparison with a salient-pole inductor is lower reactive power, respectively, lower current load (especially if, for technological reasons, the length of the inductor bore in the reactor exceeds its diameter) and the ability to reduce higher harmonics where necessary. Recently, the RMF characteristics of a reactor with a similar 42-slot inductor were calculated using the FEMM program [18]. For comparison with the FEMM results, a comparative calculation of some RMF characteristics of the specified inductor for 42 slots on Desmos was carried out using formulas (47), (48), the results of which are designated by the letters FD. Calculated parameters of the inductor: $m=3$; $p=1$; $q=7$; $\beta=1$ and $\beta=0.86$; $\rho=0.037$; $r_0=0.175$ m; $IW=950\sqrt{2}\cdot 28$ A.

The graphs of the FD calculations for the diametrical and shortened winding are shown in Fig. 7.

There are no graphical dependencies $B_\alpha(\alpha)$, $B(\alpha)$ in [18]. However, graphs $B_r(\alpha)$ are given for the radial component of induction at $r/r_0=0.943$ on the inner surface of the working chamber with a radius of 165 mm [18, Fig. 2, P. 174], which can be used for the comparison of interest to us. Comparison on the same scale showed that these graphs are almost identical to the graphs of the radial component of induction in Fig. 7, *a*, *b*. The difference in peak values is insignificant: 0.37 T FD and 0.38 T FEMM – diametrical winding; 0.288 T FD and 0.28 T FEMM – the winding pitch is shortened to 0.86.

The first harmonic induction modulus with a diametrical coil pitch according to FD (47), (48):

$$B_1=\mu_0\frac{I_m W}{r_0}\cdot\frac{m}{\pi}\left(\frac{r}{r_0}\right)^0 k_{w1}=4\pi\cdot 10^{-7}\frac{(950\cdot\sqrt{2})\cdot 28}{0.175}\times$$

$$\times\frac{3}{\pi}\cdot\frac{\sin(0.037)}{0.037}\cdot\frac{\sin(\pi/6)}{7\sin(\pi/42)}=0.246\ T.$$

When the pitch is shortened to 0.86, the induction in the center according to FD will be 0.2405 T.

The results of calculating the induction modulus at three characteristic points selected in Fig. 1 [18] are presented in Table 2.

Thus, the difference between the FD and FEMM results did not exceed 5 %. At the same time, the calculation and evaluation of the RMF of a specific inductor using the FD method takes several minutes. Special computer knowledge is not required to work with the calculator.

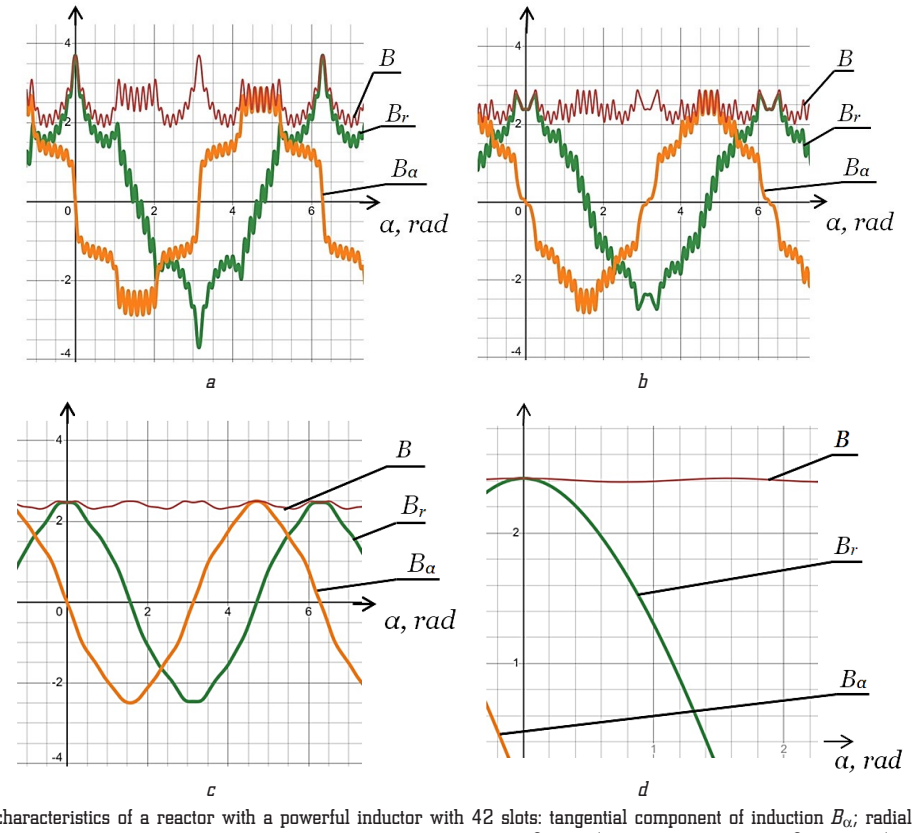

Fig. 7. RMF characteristics of a reactor with a powerful inductor with 42 slots: tangential component of induction B_α; radial component B_r; modulus of the resulting induction B; induction values are given in 0.1 T: *a* – $\beta=1$, $r/r_0=0.943$, $\omega t=0$; *b* – $\beta=0.86$, $r/r_0=0.943$, $\omega t=0$; *c* – $\beta=0.86$, $r/r_0=0.8$, $\omega t=0$; *d* – $\beta=0.86$, $r/r_0=0.5$, $\omega t=0$

ISSN 2664-9969

Table 2

Comparison of calculated induction values according to FD and FEMM

β	B_{max}, T					
	Point 1		Point 2		Point 3	
	FEMM	FD	FEMM	FD	FEMM	FD
1	0.242	0.246	0.379	0.37	0.272	0.288
0.86	0.236	0.241	0.237	0.24	0.222	0.227

Let's note that the level of higher harmonics in this reactor is significantly lower than in the reactor of *example No. 1*, which is clearly evident from the comparison of Fig. 7, *c* and Fig. 4 ($r/r_0=0.8$, $\omega t=0$). A quantitative comparative assessment of the level of higher harmonics in reactors for a less obvious case is given in *example No. 3*.

Example No. 3. A reactor with a six-phase two-pole inductor with 12 slots and a diametrical winding to create a precision uniform rotating magnetic field.

Calculation parameters for dimensionless induction calculations using FD: $m=6$; $p=1$; $q=1$; $\beta=1$, $\rho=0.043$. In the case under consideration, Gramme winding can be used to construct a six-phase diametrical winding.

The literature contains a RMF calculation of an analogue of such an inductor in the version of the Gramme winding on a toothless ferrite core for weak RMFs of a fairly high frequency. This calculation, carried out using the 2D modeling code on OPERA-2D, revealed the content of higher harmonics in the region $r/r_0 \le 0.5$ less than $5\cdot10^{-4}$ [19]. According to FD calculations, the mean square deviation of the induction vector modulus from the first harmonic vector modulus in relation to the first harmonic modulus on the radius $r/r_0=0.5$ was $7.5\cdot10^{-4}$, which agrees with the presented results of numerical modeling. A similar relative average deviation at the same relative radius by FD for the RMF of the inductor of *example No. 2* was 0.4 %, and for the inductor of *example No. 1* it was 4.5 %. As ωt scanning on Desmos shows, the average arithmetic deviation of the resulting induction modulus from the first harmonic modulus in all the cases considered depends little on the choice of the moment in time, therefore this indicator for evaluation calculations is sufficient to determine for one moment (usually $\omega t=0$).

FD graphs for the RMF characteristics of this reactor on a circle $r/r_0=0.5$ are shown in Fig. 8.

When considering *examples No. 1–3*, the adequacy of the proposed analytical formulas for estimating and analyzing the RMF of reactors with external two-pole inductors was confirmed. It is advisable to continue working on accumulating the results of applying the proposed formulas to reactors with other inductors.

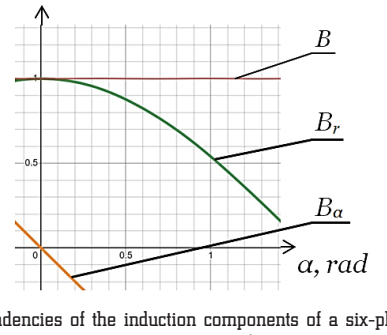

Fig. 8. Dependencies of the induction components of a six-phase inductor with a diametrical winding $r/r_0=0.5$, $\omega t=0$

Limitations: with winding asymmetry, significant saturation of steel, strong influence of the axial component of the RMF, and other circumstances causing significant deviations from the accepted assumptions, the accuracy of the formulas can decrease and should be further investigated.

In the future, it is advisable to use formulas (47)–(52) in the practice of research and design of process reactors and inductors. This can be done both in the form of the FD program and in various combinations with other computer programs, including numerical field methods. *The main areas of further application* of the new analytical formulas: fast evaluation calculations and analysis of the RMF; estimated calculations of torques and forces acting on MP and the environment in the reactor; estimated main parameters of the inductor for given requirements for the RMF density.

4. Conclusions

A mathematical model has been constructed and analytical formulas for magnetic flux density have been obtained, linking the characteristics of a quasi-stationary plane-parallel elliptical RMF density in the working zone of the process reactors' RMF with the parameters of *m*-phase cylindrical inductors of external and internal design with a longitudinal symmetric winding.

Examples of calculations and analysis of the magnetic flux density of various reactors using the obtained formulas and an easy-to-use, free DESMOS graphical calculator are given. The calculation results have been confirmed both experimentally and by comparison with available literature data. The time spent on calculations is insignificant.

It has been shown that the characteristics of the elliptical RMF of the reactors under consideration approach the characteristics of the circular field of the first harmonic of magnetic flux density when moving away from the surface of the inductor core with longitudinal windings. Near the core surface, the hodograph of the magnetic induction vector in the reactor has a strong ellipticity. At the same time, at different operating points, the hodograph ellipse has a different angle of inclination, different absolute values and axis ratios, as well as a certain spatial periodicity. These RMF features in the considered reactors can be used to implement various technologies for the impact of RMP and MP on the processed medium.

New analytical formulas, as well as the demonstrated methods of calculations, analysis and experimental studies are recommended for practical use in the design, operation and study of the considered reactors.

Acknowledgments

The work is dedicated to the blessed memory of D. D. Logvinenko – the first developer of industrial reactors with rotating magnetic fields and a vortex layer of anisotropic ferromagnetic particles for the intensification of technological processes.

Conflict of interest

The authors declare that they have no conflict of interest in relation to this research, whether financial, personal, authorship or otherwise, that could affect the research and its results presented in this paper.

Financing

The research was performed without financial support.

Data availability

An example of calculations of functional dependencies presented in Fig. 4 of this study can be viewed in the calculator cloud at the link [20]. Other files for organizing FD calculations can be provided by the authors upon separate requests.

Use of artificial intelligence

The authors confirm that they did not use artificial intelligence technologies when creating the current work.

References

1. Logvinenko, D. D., Shelyakov, O. P., Pol'shchikov, G. A. (1974). Determination of the main parameters of vortex bed apparatus. *Chemical and Petroleum Engineering, 10 (1)*, 15–17. https://doi.org/10.1007/bf01146127
2. Oberemok, V. M. (2010). Elektromahnitni aparaty z feromahnitnymy robochymy elementamy. *Osoblyvosti zastosuvannia*. Poltava: RVV PUSKU, 201. Available at: http://dspace.puet.edu.ua/handle/123456789/6536
3. *GlobeCore Transformer Oil Purification Equipment, Bitumen Equipmen*. Available at: https://globecore.com/ Last accessed: 22.09.2023
4. Kazak, O., Halbedel, B. (2023). Correlation of the Vector Gradient of a Magnetic Field with the Kinetic Energy of Hard Magnetic Milling Beads in Electromechanical Mills. *Chemie Ingenieur Technik, 95 (10)*, 1615–1622. https://doi.org/10.1002/cite.202200183
5. Ogonowski, S. (2021). On-Line Optimization of Energy Consumption in Electromagnetic Mill Installation. *Energies, 14 (9)*, 2380. https://doi.org/10.3390/en14092380
6. Ibragimov, R., Korolev, E., Potapova, L., Deberdeev, T., Khasanov, A. (2022). The Influence of Physical Activation of Portland Cement in the Electromagnetic Vortex Layer on the Structure Formation of Cement Stone: The Effect of Extended Storage Period and Carbon Nanotubes Modification. *Buildings, 12 (6)*, 711. https://doi.org/10.3390/buildings12060711
7. Litinas, A., Geivanidis, S., Faliakis, A., Courouclis, Y., Samaras, Z., Keder, A. et al. (2020). Biodiesel production from high FFA feedstocks with a novel chemical multifunctional process intensifier. *Biofuel Research Journal, 7 (2)*, 1170–1177. https://doi.org/10.18331/brj2020.7.2.5
8. Hajiani, P., Larachi, F. (2014). Magnetic-field assisted mixing of liquids using magnetic nanoparticles. *Chemical Engineering and Processing: Process Intensification, 84*, 31–37. https://doi.org/10.1016/j.cep.2014.03.012
9. Hallali, N., Rocacher, T., Crouzet, C., Béard, J., Douard, T., Khalfaoui, A. et al. (2022). Low-frequency rotating and alternating magnetic field generators for biological applications: Design details of home-made setups. *Journal of Magnetism and Magnetic Materials, 564*, 170093. https://doi.org/10.1016/j.jmmm.2022.170093
10. Polshchikov, H., Zhukov, P. (2023). Force effect of a circular rotating magnetic field of a cylindrical electric inductor on a ferromagnetic particle in process reactors. *Technology Audit and Production Reserves, 6 (1 (74))*, 34–40. https://doi.org/10.15587/2706-5448.2023.293005
11. Polshchikov, G. A., Zhukov, P. B. (1975). O dvizhenii magnitnoi chastitcy v apparate s vikhrevym sloem. *Khimicheskoe mashinostroenie (respublikanskii mezhvedomstvennyi nauchno tekhnicheskii sbornik), 22*. Kyiv: Tekhnika, 71–80.
12. Polivanov, K. M., Levitan, S. A. (1966). One problem in calculating a rotating magnetic field. *Electrotekhnika, 12*, 5–7.
13. Toirov, O., Pirmatov, N., Khalbutaeva, A., Jumaeva, D., Khamzaev, A. (2023). Method of calculation of the magnetic induction of the stator winding of a spiritual synchronous motor. *E3S Web of Conferences, 401*, 04033. https://doi.org/10.1051/e3sconf/202340104033
14. Vygodskii, M. Ia. (1973). *Spravochnik po vysshei matematike*. Nauka, 715.
15. Gradshtein, I. S., Ryzhik, I. M. (1962). *Tablitcy integralov, summ, riadov i proizvedenii*. Fizmatgiz, 43.
16. Polivanov, K. M. (1969). *Teoreticheskie osnovy elektrotekhniki, P. 3*. Energia, 338.
17. Keskiula, V. F., Ristkhein, E. M. (1965). Vozmozhnye sistemy magnitoprovoda i obmotok induktcionnykh vrashchatelei. *Trudy Tallinskogo politekhnicheskogo instituta. Seriia A, 231*, 69–85.
18. Milykh, V. I., Shilkova, L. V. (2019). Numerical-field evaluation of an efficiency of a shortening of a three-phase stator winding of a cylindrical magnetic field inductor. *Bulletin of NTU "Kharkiv Polytechnic Institute" Series: Electrical Machines and Electromechanical Energy Conversion, 20 (1345)*, 172–176. https://doi.org/10.20998/2409-9295.2019.20.25
19. Ben-Zvi, I., Chang, X., Litvinenko, V., Meng, W., Pikin, A., Skaritka, J. (2011). Generating high-frequency, rotating magnetic fields with low harmonic content. *Physical Review Special Topics – Accelerators and Beams, 14 (9)*. https://doi.org/10.1103/physrevstab.14.092001
20. *Cloud of the Desmos calculator with an example of calculating functional dependencies in Fig. 4*. Available at: https://www.desmos.com/calculator/slwa1yn5ap

✉***Henrikh Polshchikov,*** *Head of Electromagnetic Devices Sector (retired), Department of Vortex Mixing Apparatus, Private Joint Stock Company "Research and Development Institute of Enameled Chemical Equipment and New Technologies Kolan", Poltava, Ukraine, e-mail: genrikharonovich@gmail.com, ORCID: https://orcid.org/0009-0001-2197-2373*

Pavlo Zhukov, *Electrician Engineer (retired), Private Joint Stock Company "Research and Development Institute of Enameled Chemical Equipment and New Technologies Kolan", Poltava, Ukraine, ORCID: https://orcid.org/0009-0005-5661-0275*

✉*Corresponding author*